Journal of Materials Chemistry B

ROYAL SOCIETY OF CHEMISTRY

REVIEW

View Article Online
View Journal | View Issue

Cite this: J. Mater. Chem. B, 2020, 8, 3408

Aptamer-based nanostructured interfaces for the detection and release of circulating tumor cells

Pi Ding, [a] Zhili Wang, [a] Zeen Wu,[ab] Weipei Zhu,[b] Lifen Liu,[b] Na Sun*[a] and Renjun Pei *[a]

Received 3rd November 2019,
Accepted 22nd January 2020

DOI: 10.1039/c9tb02457c

rsc.li/materials-b

Analysis of circulating tumor cells (CTCs) can provide significant clinical information for tumors, which has proven to be helpful for cancer diagnosis, prognosis monitoring, treatment efficacy, and personalized therapy. However, CTCs are an extremely rare cell population, which challenges the isolation of CTCs from patient blood. Over the last few decades, many strategies for CTC detection have been developed based on the physical and biological properties of CTCs. Among them, nanostructured interfaces have been widely applied as CTC detection platforms to overcome the current limitations associated with CTC capture. Furthermore, aptamers have attracted significant attention in the detection of CTCs due to their advantages, including good affinity, low cost, easy modification, excellent stability, and low immunogenicity. In addition, effective and nondestructive release of CTCs can be achieved by aptamer-mediated methods that are used under mild conditions. Herein, we review some progress in the detection and release of CTCs through aptamer-functionalized nanostructured interfaces.

1. Introduction

Circulating tumor cells (CTCs) are a rare population of cancer cells that are shed from solid tumors and disseminate into circulating blood.[1] When CTCs travel through the circulation, they are able to remain as single cells or cluster together, and even lodge themselves into distant tissues to form new tumor sites, thereby causing tumor metastasis.[2] Metastases, the spread of cells from primary tumor sites to distant organs, and relentless growth are the most fearsome aspects of cancer, and they are the main reasons involved in the death of cancer patients.[3,4] Traditional tumor diagnosis principally depends on the biopsy of tumor tissue; however, there are some inherent limitations, including patients who are not suitable for operation, inconvenient location of the tumor, clinical risk of tissue biopsy, and tumor heterogeneity.[5] In the clinic, CTCs have been considered useful as a biomarker for early cancer diagnosis,[6,7] thereby

[a] CAS Key Laboratory of Nano-Bio Interface, Suzhou Institute of Nano-Tech and Nano-Bionics, Chinese Academy of Sciences, Suzhou 215123, China. E-mail: nsun2013@sinano.ac.cn, rjpei2011@sinano.ac.cn
[b] The Second Affiliated Hospital of Soochow University, Suzhou 215004, China

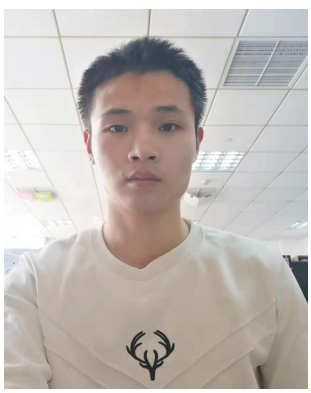

Pi Ding

Pi Ding is currently studying for his PhD degree at Suzhou Institute of Nano-Tech and Nano-Bionics, Chinese Academy of Sciences. His research is focused on using nanostructured materials to capture, isolate and release circulating tumor cells.

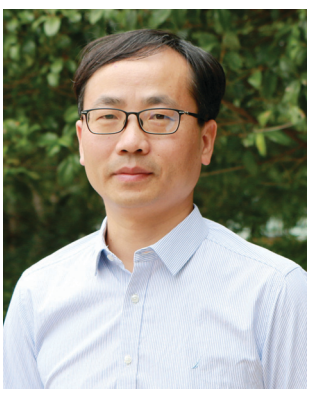

Renjun Pei

Prof. Renjun Pei received his bachelor degree and PhD from Wuhan University, and is currently working as a professor in the CAS Key Laboratory of Nano-Bio Interface, Suzhou Institute of Nano-Tech and Nano-Bionics, Chinese Academy of Sciences. His current research interests include: (1) biomaterials, injectable hydrogels and 3D bio-printing with stem cells for tissue regeneration and (2) aptamer SELEX and applications, including light-up probes, in vivo MRI probes, isolation of circulating tumor cells, and targeted delivery nano-platforms.

predicting overall survival,[8,9] drug susceptibility,[10] and prognosis monitoring.[11,12] In addition, the detection of CTCs will also further enhance diagnostic accuracy and improve the survival rate of patients.[13] In previous studies, it has been shown that the presence of 5 or more CTCs in 7.5 mL of patient blood may indicate a shorter progression-free period and overall survival.[8,14] Therefore, detection and characterization of CTCs are of great importance to provide critical information for cancer diagnosis, progression, and metastasis.

However, due to the scarcity and heterogeneity of CTCs, the analysis of them is not widely used in tumor management.[15] It should be noted that in the bloodstream of patients, the concentration of CTCs is extremely low and they are mixed with large amounts of red blood cells, white blood cells, blood platelets, *etc.*[16] One milliliter of whole blood may contain only several CTCs, while the same amount of blood has 10^9–10^{10} red blood cells and 10^6–10^7 white blood cells.[17] This makes it extremely difficult to examine and capture CTCs with high efficiency and purity. Furthermore, another significant technical problem is the heterogeneity of tumor cells.[18] The histologically genetic differentiation of different tumor types leads to diverse protein expression on the cell surface, causing the heterogeneity of tumor cells.[19] Simultaneously, the same type of tumor in different patients may lead to different levels of protein expression on the surface of the cancer cell. Furthermore, during the metastatic process, several CTCs may undergo the process of epithelial–mesenchymal transformation, which will lead to the loss some of the epithelial characteristics and the increase of some features of a mesenchymal phenotype.[20,21] Due to the heterogeneity of tumor cells, the capture and detection of CTCs may be highly dependent on the targeting molecule used in the method, which may also be a challenge for the technology that is applied in the clinic.

To overcome the above problems, over recent decades, various methods have been proposed to enrich and detect CTCs from whole blood.[22–25] These strategies have been developed prevailingly based on the differences between CTCs and hematologic cells, including physical properties (size, density, electric charges, and deformability) and biological properties (cell surface protein expression and viability).[25–27] Immunocapture based on the interaction between cancer cell surface proteins and antibody functional materials is a prevalent technique for the enrichment of CTCs. Currently, the CellSearch system is the only system validated by the US Food and Drug Administration for the detection of CTCs in patients in the clinic, which mainly utilizes anti-EpCAM antibody-functionalized magnetic particles to detect CTCs in blood of patients with metastatic breast, prostate, colorectal, pancreatic, gastrointestinal, and lung cancers.[28–30] Importantly, with the development of nanotechnology, nanostructured materials have been successfully introduced into CTC-detecting platforms, which was inspired through the surface nanostructures of cancer cells.[24,25] The nanostructure of materials can greatly enhance the interaction between cells and substrates for CTC detection, and increase the capture sensitivity and efficiency, such as nanopillars/nanowires,[31–33] nanofibers,[34,35] nanoparticles,[36,37] nanotubes,[38,39] graphene oxide (GO),[40] fractal nanostructures,[41] and nanorough-featured surfaces.[42] Moreover, in addition to antibodies, several other bioactive molecules including aptamers,[43,44] polypeptides,[45,46] E-selectin,[47–49] phenylboronic acid,[50] folic acid,[51] hyaluronic acid,[52] and tannic acid[53] have been used to improve the efficiency of CTC detection.

Aptamers are synthetic oligonucleotide ligands with high affinity and specificity for targets comparable to that of an antibody/antigen interaction.[54] They can be screened out through the SELEX (systematic evolution of ligands by exponential enrichment) technique.[55,56] Aptamers recognize specifically a variety of targets, including proteins,[57–59] small molecules,[60–66] tissues,[67] and cells.[68–70] Over the past few decades, many aptamers against biomarkers on cancer cells have been developed, including PSMA,[71] HER2,[72] CEA,[69] MUC1,[73] and EpCAM.[74,75] When compared to antibodies, an aptamer can easily be synthesized in large quantities and modified with different chemical groups.[76] An aptamer is small in size, and allows for more accurate quantification of cell membrane markers, and enhances the distinguishing capacity in identifying distinct subpopulations.[77] In addition, captured cells can be gently released using nucleases or a complementary strand of aptamers, whereas the release of antibody-based captured CTCs requires a harsh proteolytic digestion, which can damage the extracellular domains of membrane antigens and subsequently disturb the biochemistry of the cell.[32,76] In a microfluidic chip-based system, aptamers have more advantages over antibodies; for example, it is easier to label them and they are more stable for longer periods under various conditions (pH, urea, organic solvents, and detergents).[32] Herein, we summarize the methods by which aptamers are integrated with nanoparticles, nanosubstrates, and microfluidics for the isolation and detection of CTCs.

2. Aptamer-functionalized nanoparticles for CTC detection

2.1. Single-functional system

Nanoparticles have many advantages, including a small size, easily modifiable with different ligands, and high surface-to-volume ratio, which make them widely used in the detection of CTCs. In addition, the contact between nanoparticles and CTCs can greatly improve enrichment efficiency and detection sensitivity. Aptamer-functionalized nanoparticles, such as magnetic particles (MPs),[43] SiO_2,[77] and gold nanoparticles (AuNPs),[78,79] have been proven to be of great advantage in CTC enrichment. To achieve ultrahigh sensitivity and specificity for the capture of CTCs, and to facilitate downstream cellular and molecular analysis, a device called ''NanoOctopus'' was developed as shown in Fig. 1.[43] The NanoOctopus device was designed to imitate the structure of an octopus, and MPs mimicked the octopus head, whereas DNA sequences were anchored on the surface of MPs to mimic the tentacles. Each DNA sequence contained >500 repeating ''suckers'' of DNA aptamer sequences that could specifically be combined with biomarker proteins on the surface of target cells. The sensitivity and specificity were

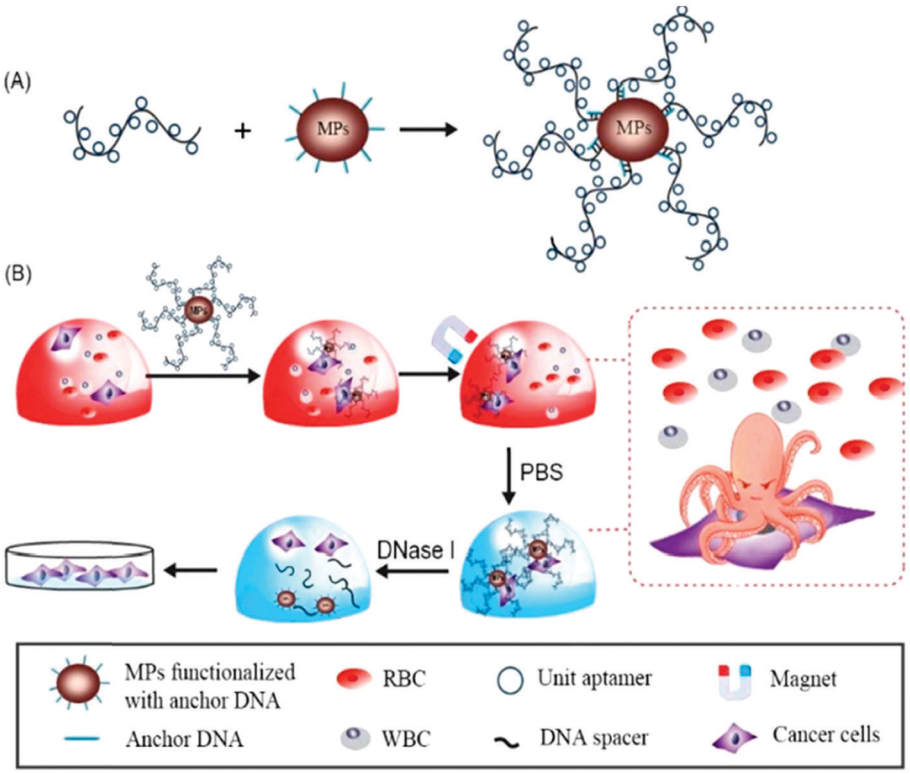

Fig. 1 The workflow of the NanoOctopus device. Aptamer-functionalized magnetic microparticles simulated the octopus head, and DNA sequences imitated the tentacles. Reprinted with permission from ref. 43. Copyright 2019, American Chemical Society.

enhanced through multivalent binding of the DNA aptamer to cell receptors without causing steric hindrance. Moreover, captured cells could be released by DNase I, which would allow for downstream cellular and molecular analysis. In a previous study, Wang *et al.* presented a virus-mimicking capture platform, which used magnetic DNA nanoclaws (MDNCs) with an octopus arm morphology to capture multiple epitopes for the enhanced capture of cancer cells.[44] The octopus arm morphology of MDNCs was generated by rolling circle amplification (RCA) and hybridized with a specific part of the tandem DNA strand of the RCA product. The structure of the DNA nanoclaws with high rigidity and flexibility could load multiple antibodies (Abs) and thereby greatly improve capture efficiency and specificity of CTCs. The capture efficiency and purity were around 95 and 85%, respectively. When antibody cocktails containing anti-EpCAM, anti-HER-2, and anti-EGFR Abs were equally conjugated on MDNCs, the capture yield of SK-BR-3 and MDA-MB-231 cells increased from 82.24 ± 2.13 to 87.74 ± 1.77%, and from 34.35 ± 1.70 to 82.3 ± 7.10%, respectively. These results strongly suggested that the synergy generated from the combined use of multiple Abs was conducive to boost the capture efficacy and specificity, thereby greatly enhancing the capture performance of triple-negative breast cancer cells. These studies showed that a DNA aptamer combined with nanoparticles could isolate the target cancer cells with high specificity and efficiency, which will open the door for the exploration of different aptamers when detecting CTCs with various types of nanoparticles.

2.2. Multifunctional system

In addition to their efficient enrichment, the identification of CTCs is also very important. Human whole blood is a complex fluid consisting of red blood cells (RBCs), white blood cells (WBCs), platelets, and other components, and especially WBCs disturb CTC identification. Some WBCs are unavoidably doped in the captured CTCs, making it essential to further identify the obtained cells for CTC detection and analysis.[80–82] In general, the captured cells are identified by immunocytochemistry, which requires the processes of cell fixation and permeabilization that can damage cell viability and cellular functions, which may also lead to CTC loss.[83,84] Therefore, a rapid and simple method for efficient capture and accurate discrimination of CTCs is highly warranted.

Two types of nanoparticles with modified aptamers were designed, with one as the capture agent to isolate CTCs, and the other as the label probe for their detection. The two-nanoparticle method was reported to rapidly isolate and detect leukemia cells using aptamers as affinity molecules.[85,86] Aptamer-functionalized magnetic nanoparticles (MNPs) were used as the capture agent, whereas other nanoparticles were simultaneously added for target cell identification. In a study by Sun *et al.*, aptamer-conjugated magnetic beads were used and surface-enhanced Raman scattering (SERS) imaging was performed to efficiently capture and accurately identify CTCs.[87] Aptamer-conjugated magnetic beads yielded a capture efficiency of 73% and 55% from buffer and whole blood samples,

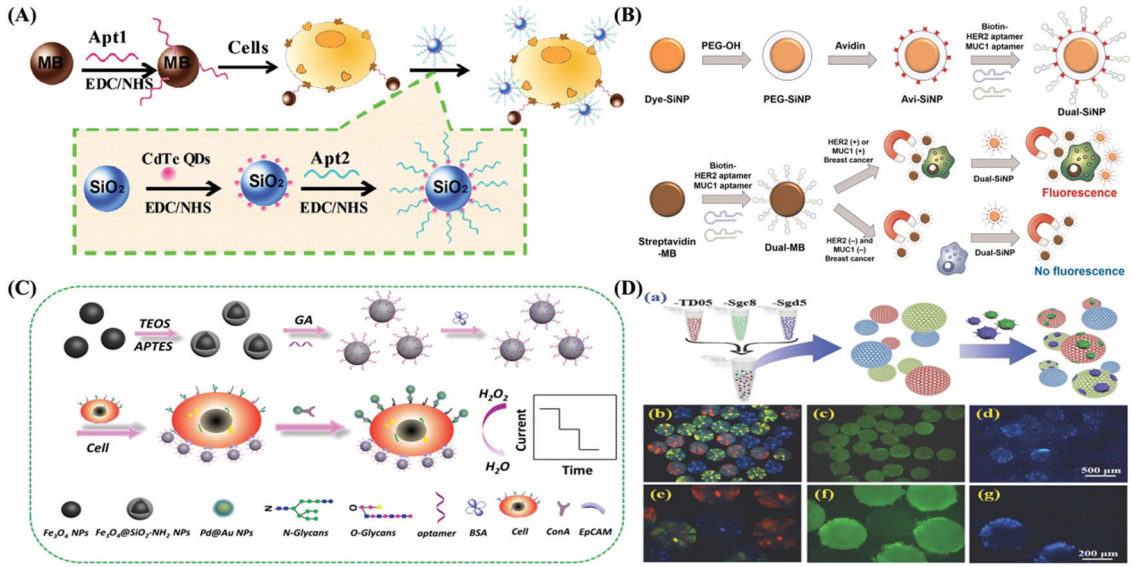

Fig. 2 (A) The isolation and detection of MCF-7 cells by employing aptamer-functionalized magnetic beads and quantum dots. Reprinted with permission from ref. 88. Copyright 2013, Elsevier BV. (B) The modification of dual aptamer-functionalized dye-SiNPs and selective detection for cancer cells. Reprinted with permission from ref. 77. Copyright 2015, Elsevier BV. (C) The fabrication and workflow of proposed electrochemical cytosensor. Reprinted with permission from ref. 79. Copyright 2019, American Chemical Society. (D) Scheme showing aptamer-functionalized barcode particles for the capture and detection of multiple types of CTCs. Reprinted with permission from ref. 95. Copyright 2014, Wiley-VCH Verlag GmbH & Co. KGaA, Weinheim.

respectively. At the same time, the captured cells were labeled with SERS probes and identified by the SERS imaging technique without the need of additional labor-intensive staining and washing procedures. Furthermore, for cellular detection, fluorescent imaging and flow cytometry were used to demonstrate the feasibility of this method. Combining the two types of nanoparticles showed rapid and sensitive detection of CTCs. In addition, another strategy was developed through aptamer-functionalized magnetic beads and quantum dot-based nanoprobes (Fig. 2A).[88] In brief, MUC1 aptamer (Apt1) was covalently conjugated to magnetic beads to capture MCF-7 cells, and CdTe quantum dots (QDs) with nucleolin aptamer AS1411 (Apt2) were coated on the surface of SiO_2 nanoparticles to form the nano-bio-probes. The probes displayed a similar optical and electrochemical performance to free CdTe QDs and high affinity remained on nucleolin-overexpressing cells. As a result, the detection limit of MCF-7 cells was 201 cells per mL by photoluminescence and 85 cells per mL by the square-wave voltammetric assay. Moreover, the selectivity was improved by using the two aptamers together as recognition elements. In fact, the isolation of CTCs may not be sensitive enough because of the heterogeneity of tumor cells. To solve the problem, two or more aptamers against cancer cells for a wide-ranging diagnosis of cancer could be used. Jo *et al.* simultaneously used two aptamers against mucin 1 (MUC1) and human epidermal growth factor receptor 2 (HER2) to modify silica nanoparticles (SiNPs) and magnetic beads (MBs) for the detection of CTCs (Fig. 2B).[77] The dye-doped SiNPs were used as the detection probe with high photostability, low-cost synthesis, great fluorescent signal, and good biocompatibility. Together, these results showed that the dual aptamer system enabled a broad diagnosis for breast cancer when compared with the single aptamer system, and displayed high selectivity and sensitivity, with a detection limit of 1 cell/100 μL. Electrochemical detection technology plays an important role in the development of sensors because of its good selectivity, high sensitivity, rapidity, simplicity, and low test cost. Liu *et al.* fabricated an electrochemical cytosensor, which could detect not only CTCs but also expression dynamic of N-glycan on CTC surfaces (Fig. 2C).[79] An aminated-SYL3C aptamer against the epithelial cell adhesion molecule (EpCAM) was attached to the surface of Fe_3O_4@SiO_2 nanoparticles through a cross-linked reaction *via* glutaraldehyde to selectively isolate target cells. Concanavalin A that specifically recognizes N-glycan carbohydrates expressed on the surface of the target cell was assembled onto Pd@AuNPs, which acted as a signal amplification probe by catalyzing the reduction of hydrogen peroxide (H_2O_2) for the detection of target cells. The detection limit is 10 cells/100 μL. In addition, Miao *et al.* were the first to develop a multipedal DNA walker for ultrasensitive detection of CTCs, in which walker strands were modified on AuNPs and an integrated aptamer sequence would bind the CTC biomarker, thereby resulting in the enrichment of AuNPs on the cell surface. After low-speed centrifugation, CTC and AuNPs complex was precipitated and the supernatant represented the decreased UV-visible absorption response of AuNPs. On the other hand, since multiple walker strands are modified on single AuNPs, hybridization with several tracks on the electrode occurs simultaneously for subsequent nicking endonuclease-catalyzed cleaving. By comparing the variations of electrochemical and UV-visible absorption responses, high sensitivity was achieved for the CTC assay (the detection limit was down to 1 cell per mL).[89] Fang *et al.* used aptamer-conjugated upconversion nanoparticles

to recognize tumor cells, which were then enriched by MNPs.[90] Due to the autofluorescence-free nature of upconversion luminescence imaging, as well as the use of magnetic separation to further reduce background signals, the method allowed for highly sensitive detection and collection of rare target cells from artificial samples.

Moreover, some nanoparticles, when assisted by modified aptamers, have been shown to isolate and identify cells simultaneously. Fluorescent-magnetic nanobeads presented a good QD fluorescent property and a strong MNP magnetic response, which is promising for the detection of CTCs.[91] Li *et al.* fabricated DNA-templated magnetic nanoparticle-QD-aptamer copolymers (MQAPs) for the isolation of CTCs from human blood samples with high capture efficiency and purity approaching 80%.[92] The phenotype of CTCs was simultaneously profiled with QD photoluminescence at the single-cell level. MQAPs were constructed through a hybridization chain reaction. The phenotype of CTCs was simultaneously profiled with QD photoluminescence at the single-cell level. Yang *et al.* reported an aptamer-based dual-functional probe for the counting and visualization of MCF-7 cells by inductively coupled plasma mass spectrometry (ICP-MS) and fluorescence imaging.[93] The probe was composed of three parts. The aptamer was used to specifically capture cancer cells, a fluorescent dye (FAM) moiety was applied for fluorescence resonance energy transfer (FRET)-based "off–on" fluorescence imaging, and a AuNPs tag was implemented for both ICP-MS quantification and fluorescence quenching. Due to the signal amplification and low spectral interference of AuNPs in ICP-MS, excellent linearity and sensitivity were achieved with a detection limit of 81 MCF-7 cells and a dynamic linear range of 2×10^2 to 1.2×10^4 cells. Lu *et al.* were the first to report a colorimetric and highly sensitive two-photon scattering assay.[94] Breast cancer cells were detected at 100 cells per mL by using a monoclonal anti-HER2 antibody and S6 RNA aptamer-conjugated oval-shaped AuNPs. When the multifunctional oval-shaped AuNPs were mixed with SK-BR-3 cells, the oval-shaped AuNPs bound to HER2 receptors that were expressed on the cancer cells, thereby producing nanoparticle aggregates resulting in a distinct color change (from pink to bluish) and a new broad band appeared around 150 nm far from the plasmon absorption band. The two-photon scattering intensity increased by about 13-fold. With the increasing demand for multiplex and high-throughput analysis, multiplex technology has become a promising tool for thousands of individual reactions simultaneously for large-scale biological analysis. Among current technologies, suspension arrays based on appropriate barcode particles have the ability of unique encoding, and are used in multiplex bioassays in many research fields, including clinical, medicinal, nutritional, and environmental fields. Zheng *et al.* developed an aptamer-functionalized barcode platform (Fig. 2D).[95] Those barcode particles were fabricated by evaporation of droplet templates containing monodisperse silica nanoparticles. The nanoparticles of the barcode particles mainly formed a close-packed colloidal crystal array structure, and the barcode particles were assembled with different diameters of silica nanoparticles. The barcode particles with different reflection peaks from 400 nm to 800 nm and their color change from blue to green to final red were reported. However, the capture efficiency of cells on barcode particles was limited due to the small number of chemical groups present on the silica surface, and the effect of the nanopatterned surface topography. To overcome these issues, barcode particles were etched to form a cell-preferred non-close-packed spherical array surface topography, and were decorated with highly branched dendrimer-amplified aptamer probes to improve capture efficiency. After interacting with aptamer-functionalized barcode particles, the capture efficiencies of Ramos and CCRF-CEM cells were up to 98% and 97%, respectively. Unlike the single-functional nanoparticle systems, these multifunctional nanoparticles integrated various functions into one system, thereby greatly expanding their applications of isolation, detection, and manipulation of target tumor cells, and decreasing the operation time.

3. Aptamer-modified nanostructured interfaces for CTC isolation

3.1. Based on a "hard substrate"

In recent decades, it has been noted that micro-/nanostructures on the surface of capture substrates can significantly enhance interactions between cells and substrates, including cell adhesion, proliferation, migration, and differentiation. Many antibody-functionalized micro-/nanostructures have been used to isolate and enrich CTCs. However, antibody-based isolations have certain limitations due to the antibody characteristics. Introduction of aptamers has attracted much attention because of their advantages, including ease of synthesis and modification, high stability, small size, low immunogenicity, and high affinity.[54–56] Therefore, aptamers are modified onto the surface of nanostructured substrates for directly capturing CTCs without the requirement of magnetic separation. Wang *et al.* developed a rough gold nanoparticle layer (GNPLs) substrate, which was modified with TD05 aptamers (GNPL-APT) (Fig. 3A).[96] Poly(oligo(ethylene glycol)methacrylate) (POEGMA) was introduced between aptamer and micro-/nanostructured surfaces as an antifouling spacer. The results showed that the density of Ramos cells that adhered to highly rough GNPL-APT substrates was 19-fold that of CEM cells. Sun *et al.* fabricated a TiO_2 nanorod array using the hydrothermal synthesis method.[97] In brief, nanorods were densely packed on F-doped SnO_2 substrates with a diameter of 160–300 nm, and some nanoparticles (diameter: 30–50 nm) were formed on the top of the nanorods, which enhanced the topographic interaction between nanoscale structures on cell surfaces and the TiO_2 nanorod array (Fig. 3B). Bovine serum albumin (BSA) was introduced into the interfaces, as an antifouling molecule, to inhibit nonspecific cell adhesion. Subsequently, aptamers were modified on the BSA of the TiO_2 nanorod array. Finally, an excellent capture yield was obtained of MCF-7 cells on the TiO_2 substrates, which was up to 85–95%. Li *et al.* integrated peptides and aptamer-S2.1 on nanowires to develop a capture platform with a high capture efficiency for MUC1-positive

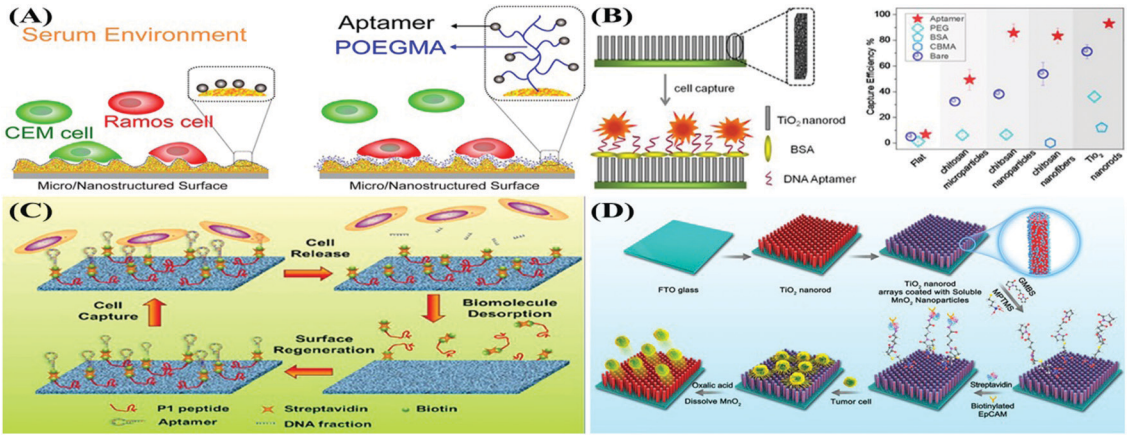

Fig. 3 (A) Aptamer-modified micro-/nanostructured surfaces for the capture of Ramos cells in serum environment. Reprinted with permission from ref. 96. Copyright 2013, American Chemical Society. (B) A uniform TiO_2 nanorod array to capture CTCs. Reprinted with permission from ref. 97. Copyright 2016, American Chemical Society. (C) Recognition and capture platform based on GaN nanowires functionalized with aptamer. Reprinted with permission from ref. 98. Copyright 2016, American Chemical Society. (D) TiO_2 nanorod arrays coated with MnO_2 nanoparticles to capture and release CTCs. Reprinted with permission from ref. 100. Copyright 2018, American Chemical Society.

cancer cells (Fig. 3C).[98] GaN nanowire surfaces were fabricated by the chemical vapor deposition method, and the peptide bio-P1 was connected with nanowires by affinity between GaN and P1, then the aptamer was connected to bio-P1 through streptavidin. The ratio of MCF-7 cells in a mixed cell suspension of MCF-7 and Ramos cells was higher than 90%. Release of captured cells was achieved by DNase, and after incubation with DNase, 98% of the captured MCF7 cells were released from the surface. The substrate surface could be regenerated by treatment with NaCl and desorbing peptide P1. Xue *et al.* reported for the first time silicon nanowire arrays (SiNWAs) to capture Ramos cells through single electron transfer living radical polymerization and click chemistry.[99] The glycopolymers were able to interact with glucose transporters that were overexpressed on cancer cell membranes. TD05 aptamers possess high affinity to Ramos cells, and were coated onto the surface of SiNWAs, thereby generating a synergistic effect for the capture of cancer cells, and as a result, a multivalency-enhanced capture was achieved of more than 60-fold over the SN–OH surface. Li *et al.* prepared a TiO_2 nanorod array by using hydrothermal synthesis, which was coated with transparent MnO_2 nanoparticles.[100] MnO_2 nanoparticles were fabricated through *in situ* self-assembly on the substrate to form a monolayer, and were etched by oxalic acid with low concentration at room temperature (Fig. 3D). The capture yield of target cells was 92.9%, about 89.9% of the captured cells could be released from the platform, and the viability of MCF-7 cancer cells exceeded 90%.

3.2. Based on a "soft substrate"

Most studies have focused on inorganic materials due to the restraints of fabrication techniques for "soft" nanostructures, which better match the soft nature of cells to retain their viability. The softness of synthetic materials greatly influences cellular processes, including cell adhesion and spreading, stem-cell proliferation and differentiation, and even tumor development. Therefore, exploring the integration of soft materials with certain chemical and physical attributes to mimic the natural microenvironment of the cell will be instructive for realizing a high-quality cell-capture platform. Chitosan is the product of the removal of some of the acetyl groups from natural polysaccharide chitin, which has many physiological features, such as biodegradability, biocompatibility, non-toxicity, and bacteriostasis.[101] Sun *et al.* developed a chitosan nanoparticle surface by electrospray.[101] The surface was modified by polyethylene glycol and a DNA aptamer for specific capture of viable rare CTCs from artificial samples. Moreover, the captured cells were further purified and proliferated through *in situ* culture. Furthermore, a chitosan nanofiber substrate was fabricated by electrospinning (Fig. 4A).[102] Poly(carboxybetaine methacrylate) (pCBMA) brushes were integrated into the nanofiber interface to provide antifouling capacity for reducing nonspecific cell adsorption, and to build a flexible space for biomolecules. Then, DNA aptamers, directed against epithelial cell adhesion molecule (EpCAM), were incorporated into the pCBMA brushes to form a multivalent agent to induce cell capture with high efficiency and specificity. The capture efficiency of spiked KATO III cells reached 53.8–66.5%, and a very small number of blood cells were observed on the substrates. Moreover, a cell-imprinted hydrogel was modified with aptamers to achieve specific capture of CTCs (Fig. 4B).[103] The substrate was imprinted by cells which not only generated recognition sites that matched the conformation and properties of the target cells, but were also used as efficient scaffolds for the assembly of aptamers to enhance the capture efficiency and selectivity. Due to the synergistic effect of conformation recognition and multivalent interaction between aptamers and target cells, the device showed a high capture efficiency and selectivity to target cells. Li *et al.* fabricated a hydrogel-coated glass substrate with high resistance to nonspecific cell binding with 5–15 cells per mm^2. However, under the same conditions, the aptamer-functionalized hydrogel coating could target cancer cells with a density over 1000 cells per mm.[2,104] Nellore *et al.* fabricated a porous GO membrane that was modified

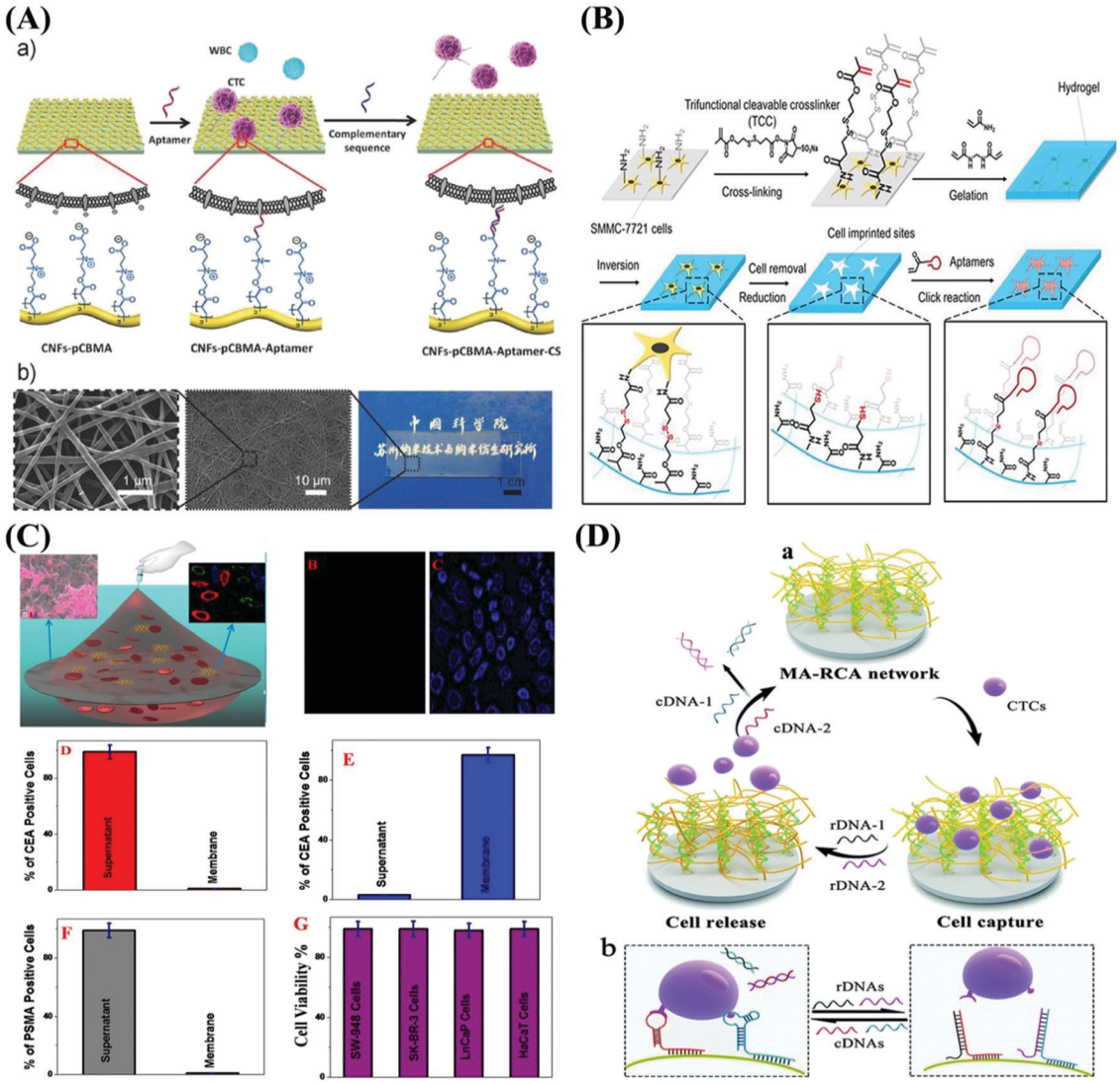

Fig. 4 (A) Chitosan nanofiber interface for the capture and nondestructive release of CTCs. Reprinted with permission from ref. 102. Copyright 2016, Wiley-VCH Verlag GmbH & Co. KGaA, Weinheim. (B) Schematic of cell-imprinted hydrogel with the site-directed modification of aptamers (APT-CIH) for capture and release of SMMC-7721 cells. Reprinted with permission from ref. 103. Copyright 2019, American Chemical Society. (C) Aptamer-conjugated 3D GO membrane for capturing multiple CTCs. Reprinted with permission from ref. 105. Copyright 2015, American Chemical Society. (D) Schematic of MA-RCA network for the capture and release of CTCs. Reproduced from ref. 107 with permission of the Royal Society of Chemistry.

with multiple aptamers (S6, A9, and YJ-1) to highly efficiently capture and accurately identify multiple types of CTCs from infected blood (Fig. 4C).[105] Three-dimensional (3D) GO was fabricated in two steps: first, two-dimensional (2D) GO sheets were obtained, and four different types of aptamers were attached on the 2D GO using a modified Hummers' method. Then polyethylene glycol was used as a cross-linking agent between 2D GO to form 3D GO. Finally, the capture efficiency of GO membranes reached 95% for SKBR3, LNCaP, and SW-948 cancer cells and identified with dye-conjugated aptamer by utilizing the fluorescence quenching properties of GO. In addition, a GO-based biosensor has also been reported for *in situ* detection of cancer cells.[106] FAM-Sgc8 was used as a model of the 'signal-on' molecular probes. In a free state, the FRET probe of GO/FAM-Sgc8 exhibited a quenched fluorescence because of p–p stacking interactions between FAM-Sgc8 and GO, whereas once target cells were introduced, the interaction between FAM-Sgc8 and CCRF-CEM cells was strong enough to release FAM-Sgc8 from GO, thereby recovering the fluorescence. A DNA network was also used as a highly effective CTC capture platform, which was fabricated by dual-aptamer-tethered rolling circle amplification (MA-RCA) based on DNA assembly (Fig. 4D).[107] The RCA strands with dual aptamers resulted in a soft multivalent binding DNA network for efficient cell capture with great extensibility and flexibility. The MA-RCA network was designed by two different aptamer interval hybrids to a long DNA scaffold with periodic sequence units generated by RCA. The multivalent binding sites endowed the MA-RCA network with a strong binding ability towards CTCs. Finally, the capture efficiency was 78 ± 8%, and more than 90% of trapped CEM cells were successfully released

after treatment with the release DNAs. Ou *et al.* developed a sandwich-type cytosensor to analyze cancer cells, which was based on the metal organic framework PCN-224 and a DNA tetrahedron linked aptamer.[108] For the first time, a metal organic framework, PCN-224, was introduced as a nanocarrier. The tetrahedral DNA nanostructures linked dual aptamers (AS1411 and MUC1), and were immobilized on a gold electrode surface as bio-recognition elements that could capture MCF-7 cells. The PCN-224 probe was homogeneously decorated with Pt nanoparticles, and modified with G-quadruplex/hemin DNAzyme, horseradish peroxidase, and a dual aptamer. Finally, this cytosensor could detect 20–10^7 cell per mL, and captured cells were released by electrochemical reductive desorption to break the Au–S bond.

4. Aptamer-modified microfluidic platforms for CTC capture

4.1. Simple microfluidic chip

Microfluidic devices have drawn significant attention in the isolation and detection of CTCs for their advantages, including small sample volume, low cost, automation, and easy integration with other techniques. Over the last decade, various microfluidic platforms have been used for microfluidic flow cytometry,[109] continuous size-based separation,[110,111] and chromatographic separation.[112] Phillips *et al.* firstly used an aptamer-functionalized microfluidic channel to enrich cancer cells.[113] The sample flowed through the channel, yielding >97% of capture purity and >80% of capture efficiency for target cells. A biomimetic microfluidic system was developed by combining the unique benefits of biomimetic nanoparticles and microfluidic techniques.[104] Magnetic nanoclusters were coated with leukocyte membrane fragments and decorated with aptamer SYL3C that was specific for EpCAM positive tumor cells, then loaded into the microfluidic chip with the help of magnets.[114] It is known that the concentration of immobilized aptamers can affect the cell isolation efficacy.[79] In addition, the competition of surface-grafted aptamers to bind cell membranes against the drag force from the fluid flow is an important factor that helps to determine the efficiency for the capture of CTCs. Wan *et al.* studied the effect of flow velocity in a microfluidic channel for isolating CTCs using an EGFR aptamer-modified device (Fig. 5A).[115] Their work showed interdependence between the adhesion probability, isolation efficiency, and flow rate, and can assist in designing flow-through lab-on-chip devices that use surface-bound probe affinities against overexpressed biomarkers for cell isolation. They also developed an aptamer-functionalized glass bead array in a channel. The Hele–Shaw channel possesses many pits, with aptamer beads sited in a polydimethylsiloxane (PDMS) channel and when a cell solution flowed through the device, cancer cells were captured with high selectivity. Cell-bound glass beads were then re-suspended from the device surface, followed by the release of 92% of cells from the glass beads using a combination of gentle shaking and anti-sense RNA.[116]

To improve the affinity of tumor cell capture by aptamers, a nanotextured PDMS substrate was developed. Nanotextured PDMS increased the surface roughness at the nanoscale and the effective surface area. The density of the immobilized EGFR-specific RNA aptamer was increased, which resulted in a higher capture efficiency to isolate cancer cells from a sample.[117] Sheng *et al.* developed an aptamer-mediated, micropillar-based microfluidic device to isolate tumor cells from unprocessed whole blood (Fig. 5B).[118] The micropillars in the microchannel were fabricated by a chemical etching method and were functionalized with aptamers. By combining the advantages of aptamer-modified nanostructures and the microfluidic device, the device yielded a capture efficiency of ~95% with a purity of ~81%, and at the optimum flow rate, as few as 10 tumor cells were captured from 1 mL of whole blood. Wang *et al.* developed a new-generation NanoVelcro chip.[32] Two aptamers were coated on silicon nanowire substrates (SiNWS), which were utilized to immobilize CTCs in a stationary device setting (Fig. 6A). Then, the SiNWS was integrated with a PDMS-based chaotic mixer that enhanced the contact frequency between flow-through cancer cells and the substrate, thereby improving the capture efficiency of CTCs. At optimized conditions, the capture efficiency exceeded 80% for A549 cells in artificial blood samples, and the release efficiency was more than 85%.[32] To improve the enrichment of multiple cancer cells, aptamer cocktails were introduced into a NanoVelcro chip by Zhao *et al.*[119] The microfluidic chip was composed of an aptamer-grafted SiNWS

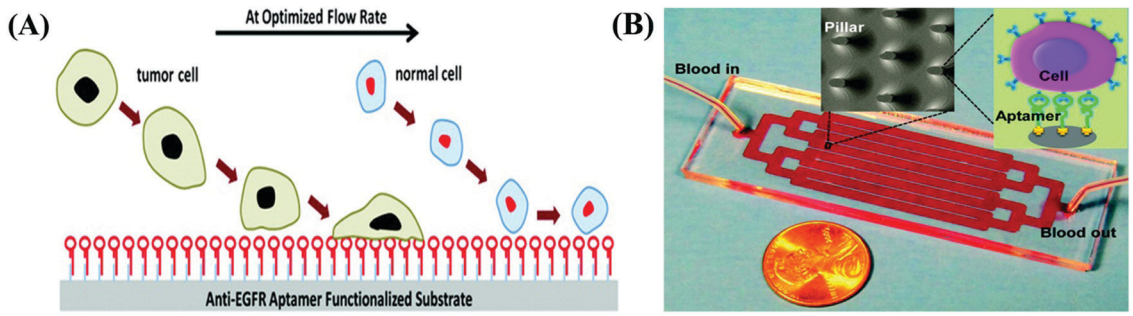

Fig. 5 (A) The aptamer against EGFR modified device for isolating cancer cells from laminar flow of sample. Reprinted with permission from ref. 115. Copyright 2011, American Chemical Society. (B) Aptamer-mediated, micropillar-based microfluidic device for CTC detection. Reprinted with permission from ref. 118. Copyright 2012, American Chemical Society.

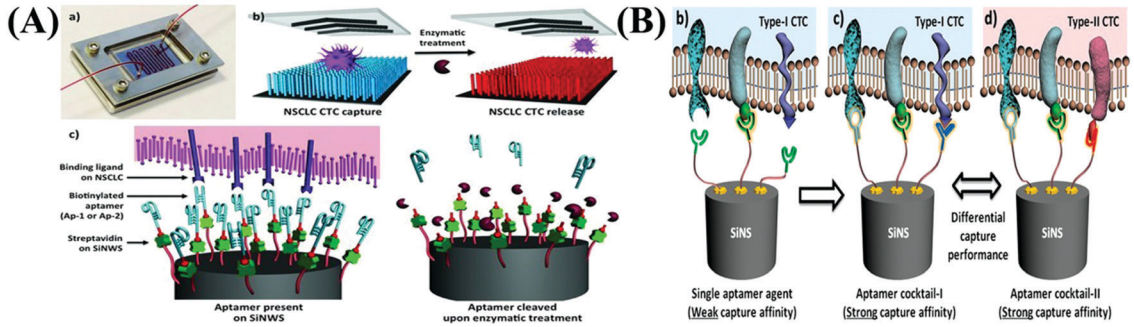

Fig. 6 (A) NanoVelcro chip consisting of aptamer-coated silicon nanowire substrate (SiNWS) and an overlaid PDMS chaotic mixer. Reprinted with permission from ref. 32. Copyright 2013, Wiley-VCH Verlag GmbH & Co. KGaA, Weinheim. (B) Microfluidic CTC chip based on aptamer cocktail-grafted SiNWS. Reprinted with permission from ref. 119. Copyright 2016, Wiley-VCH Verlag GmbH & Co. KGaA, Weinheim.

and an overlaid PDMS chaotic mixer (Fig. 6B). When a single aptamer as capture agent was employed, the capture affinity of the device was relatively weak for the lack of synergistic binding. With synergistic effects, the cocktail showed >50% capture performance across all five non-small-cell lung cancer cell lines.

4.2. Multifunctional microfluidic chip

Microfluidic isolation and the analysis of cells have been the focus of studies in past decades, including CTC isolation, single-cell analysis, and stem cell separation. Furthermore, 3D nanostructured substrates have been integrated into microfluidic channels,[32] which improved the capture efficiency *via* local topographic interactions between the interface and cell-surface components. To simplify the experimental process and improve isolation efficiency, many multi-purpose and multi-function microfluidic devices have been developed.[120–128] For the capture of cancer cells, Song *et al.* fabricated a deterministic lateral displacement (DLD) microfluidic chip, which was functionalized with aptamer-conjugated nanospheres (AP-octopus-chip) (Fig. 7A).[120] To improve the capture efficiency, a size-dictated immunocapture

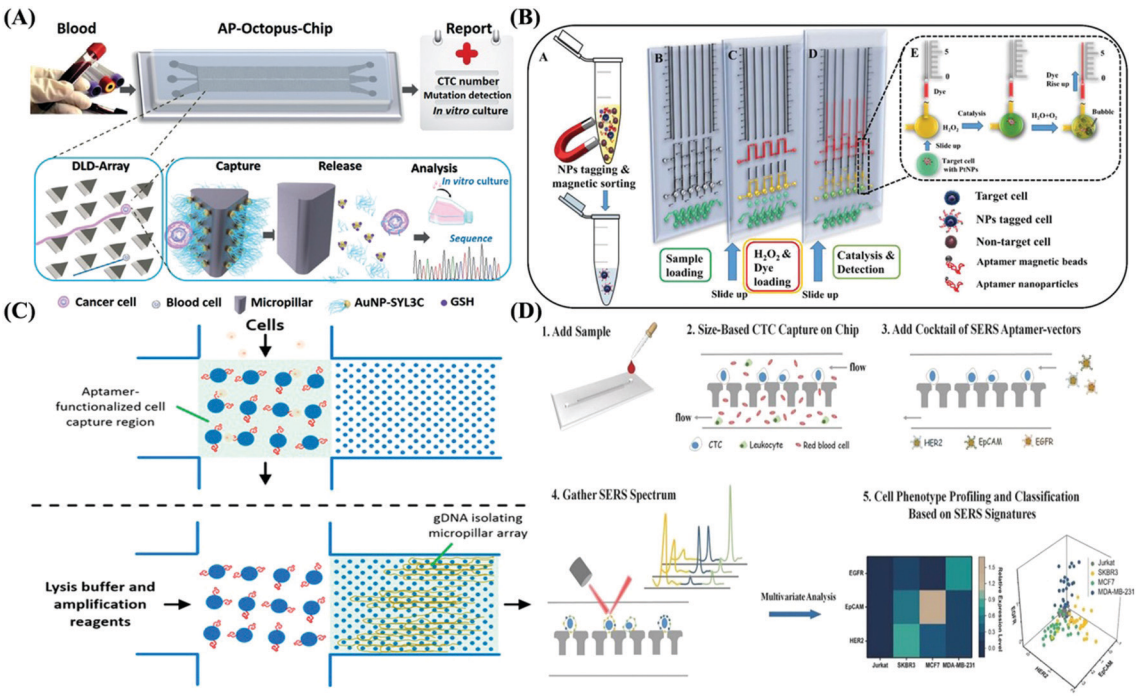

Fig. 7 (A) Working principle of the AP-octopus-chip. When a sample is passed through the channel, the CTCs interact with AuNP–SYL3C-modified micropillar based on the DLD principle. While smaller blood cells would remain within the original flow streamline. The captured CTCs could be released by Au@S bond disruption by excess GSH. Reprinted with permission from ref. 120. Copyright 2019 Wiley-VCH Verlag GmbH & Co. KGaA, Weinheim. (B) The workflow of the aptamer-conjugated volumetric bar chart chip readout for the visual quantifiable detection of CTCs. Reprinted with permission from ref. 122. Copyright 2019, Wiley-VCH Verlag GmbH & Co. KGaA, Weinheim. (C) Multifunction device which could capture cancer cells and isolate their gDNA for specific amplification and sequence analysis. Reprinted with permission from ref. 123. Copyright 2018, American Chemical Society. (D) Workflow of operation on a platform for CTC capture, profiling of cell phenotype, and classification based on SERS signatures. Reprinted with permission from ref. 125. Copyright 2018, Wiley-VCH Verlag GmbH & Co. KGaA, Weinheim.

chip (SDIChip) was integrated with a multivalent aptamer nanointerface. AuNPs as scaffolds were modified with multivalent aptamers (SYL3C) through the Au–S bond, resulting in a 100-fold higher binding affinity, when compared to monovalent SYL3C, between SYL3C–AuNPs and SW480 cells. Samples flowed through an AP-octopus-chip and interacted with an AuNP–SYL3C-modified micropillar. WBCs, which are smaller than CTCs, remained within the original flow streamline, and had a low interaction probability. After capturing, the enriched CTCs could be released through Au@S bond disruption by an excess of GSH, which was fully compatible with downstream analysis. Recently, a variety of aptamer sensors have been developed. Liu *et al.* reported an aptamer probe, which showed strong potential for breast cancer diagnostics and therapy.[121] Aptamers against SK-BR-3 were evolved by Cell-SELEX. After 21 rounds of *in vitro* selection and sequence truncation, an aptamer-based probe, sk6Ea, was obtained. This probe distinguished SK-BR-3 cells from different subtypes of breast cancer cells and normal human mammary epithelial cells. Furthermore, using this probe, HER2-enriched breast cancer could also be differentiated from three other breast cancer subtypes and adjacent normal breast tissues. Abate *et al.* designed a volumetric bar chart chip (V-Chip) for visual quantitative detection of CTCs at the single-cell level (Fig. 7B).[122] Target CTCs were labeled with aptamer-conjugated nanoparticles (ACNPs) and quantified by the catalytic reaction between bound ACNPs and H_2O_2 to translate the CTC number into readily visually detectable information. Single-cell detection could be realized; however, the efficiency may be compromised in the presence of a high leukocyte background. The device with potential could be further exploited using quantitative detection of any biological samples by simply integrating any simple enrichment method, such as magnetic sorting of target cells, from several background samples. Reinholt *et al.* developed a multifunction device, which captured cancer cells and isolated their genomic DNA (gDNA) (Fig. 7C).[123] This device consisted of two orthogonal channels, namely the cell channel and the DNA channel. It also contained two micropillar arrays: the cell capture array located at the intersection of the channels and the DNA isolation array located downstream of the cell capture array in the DNA channel. To enhance the capture efficiency, the aptamers were modified onto the channel, the captured cells were lysed *in situ*, and the gDNA was isolated by physical entanglement and amplified using a modified version of the multiple displacement amplification technique. Dharmasiri *et al.* developed a PMMA microchip.[124] Anti-prostate-specific membrane antigen aptamers were immobilized onto the surface of the capture bed, and fabricated into a high-throughput microsampling unit that was used for the selective isolation of CTCs that were resident in a peripheral blood matrix. Prostate-specific CTCs could be isolated from whole blood and no sample pretreatment was necessary. The enumeration of CTCs did not need staining but was achieved through a Pt conductivity sensor. Zhang *et al.* reported an *in situ* isolating and profiling CTC microfluidic chip (Fig. 7D).[125] Tumor cells were sieved from blood based on size discrepancy, and three types of spectrally orthogonal SERS aptamers were designed to analyze cancer subpopulations. When samples containing cancer cells passed through the microfluidic device, the larger CTCs could be efficiently captured by the two "shoulder" structures, while contaminating blood cells were filtered out. Then, three aptamer–Au@Ag nanoparticles were added to acquire a SERS signature for each cell. Finally, the revised classic least squares algorithm and partial least squares discriminate analysis were used to accurately categorize cells with different subtypes. Sun *et al.* proposed a size enlargement method, which utilized aptamer-modified microbeads to increase capture efficiency for the target cells.[126] Microbeads modified with an aptamer would react with CTCs and enlarge in size, which entrapped smaller CTCs on polycarbonate membranes and increased capture efficiency. Moreover, a WBC depletion process was introduced to decrease WBCs that were retained on the filter membrane.[126] Apart from CTCs, exosomes have drawn significant attention, containing a large variety of proteins, nucleic acids, and lipids, and were recognized as promising sources of biomarkers for early cancer diagnosis. Therefore, the development of a sensitive and low-cost detection method for exosomes is highly desirable. Yu *et al.* reported an exosome competitive fluorescence detection method based on CD63 aptamers.[127] First, aptamers were hybridized with the Cy3-labeled short complementary sequence, then after the sample containing the exosomes was added, the short sequence would shed into the supernatant for competitive binding of CD63 on the exosomes. The content of exosomes can be indirectly estimated by detecting the fluorescence intensity in the supernatant. The limit of detection of this method was as low as 1.0×10^5 particles per μL, which was much lower compared to the normal level of exosomes in serum. A label-free electrochemical aptasensor was also developed to determine gastric cancer-specific exosomes.[128] The gastric cancer exosome-specific aptamer probe was selected and linked to a primer sequence that was complementary to a G-quadruplex circular template. After exosomes were captured by an anti-CD-63 antibody, only gastric cancer exosomes could trigger RCA to generate large amounts of G-quadruplex units. Finally, an electrochemical signal was produced by the catalysis of H_2O_2 system.

5. Aptamer-mediated release for captured CTCs

5.1. Complementary sequence displacement

The release of viable cells is necessary for downstream analyses, including cell proliferation, drug sensitivity tests, and whole genome sequencing, which are critical for understanding the mechanism underlying tumor metastasis. To release captured cells without damage, many strategies have been proposed, including enzymatic hydrolysis,[32,106,129,130] temperature-controlled release,[131] shear stress-mediated elution,[132–134] photochemical bond breaking,[135,136] and chemical competitive binding.[50,137] The methods mentioned above sometimes cause damage to the released cells. The release process on aptamer modified platforms can be gentle by changing the secondary structure of aptamers *via* nuclease degradation[106,129] or complementary

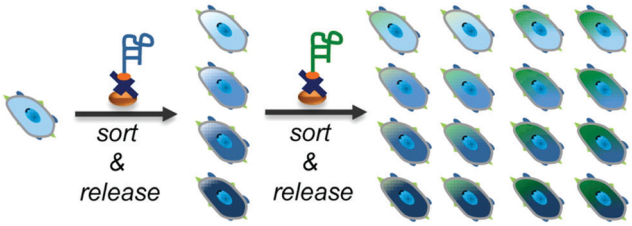

Fig. 8 Schematic of the 2D sorting chip. Cells were tagged with aptamer-modified magnetic nanoparticles specific to the first surface marker and sorted into four subpopulations using a fluidic device. The four subpopulations were then released using a complementary antisense DNA strand and subsequently tagged with magnetic nanoparticles labeled with an aptamer specific to the second surface marker. After sorting the captured cells into 16 subpopulations, cells were released using the complementary DNA strand to the second aptamer. Reprinted with permission from ref. 138. Copyright 2016, American Chemical Society.

sequence displacement.[101,138–140] Labib *et al.* reported an aptamer-mediated, 2D approach that isolated cancer cell subpopulations using a fluidic chip (Fig. 8).[138] The chip contained X-shaped structures that generated localized pockets of low velocity that favored the accumulation of nanoparticle-tagged cells. Cells that highly expressed the cell surface marker were captured in the first zone, whereas cells with medium to low expression levels were trapped in later zones. Using this approach, cells were sorted into four subpopulations. The four subpopulations were released by using a complementary DNA strand, and were subsequently tagged with MNPs modified with an aptamer that specifically bound the second surface marker. After sorting the captured cells into 16 subpopulations, cells were released by the complementary strand of the second aptamer. Therefore, CTCs were sorted from the different subpopulations based on the expression level of two surface markers. The maximum level of capture was aptamer dependent, with the EGFR1 aptamer producing the highest level of capture that approached 90%. Release efficiencies approaching 80% were achieved under optimized conditions. Other methods were also developed, and the captured cells on a hydrogel surface could be programmed by using hybridized aptamers and triggering complementary sequences (CSs). In the absence of triggering CSs, aptamers exhibited a stable, hybridized state in the hydrogel for a cell-type-specific capture. In the presence of the triggering CSs, aptamers were transformed into a new hybridized state that resulted in rapid dissociation of the aptamers from the hydrogel. The cell release kinetics showed that more than 95% of the cells were released within the first 10 min.[139]

5.2. Nuclease cleavage

Compared with protease-treated mediated CTC release, nucleases degraded aptamers, which did not destroy the surface proteins of cell membranes, and had little effect on cell viability. Zhao *et al.* developed a CTC capture platform using 3D DNA networks, which consisted of repeating aptamer domains (Fig. 9).[129] The DNA network was synthesized by RCA, and after integration with a herringbone microfluidic device, the capture efficiency was significantly improved. After DNase I was

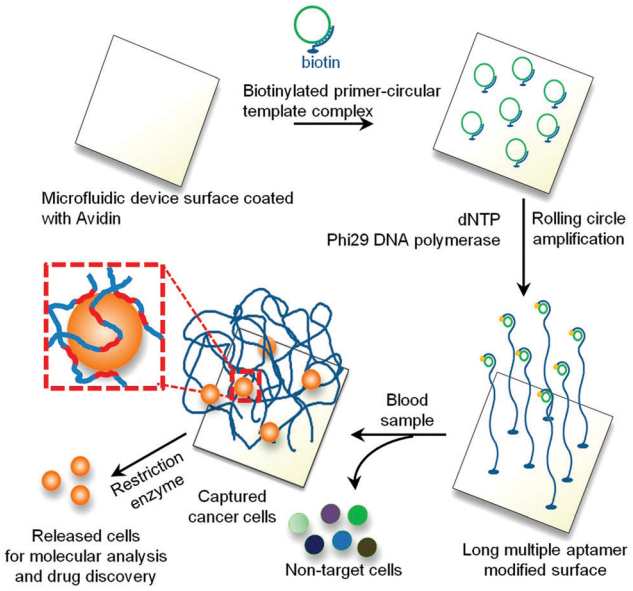

Fig. 9 Capture and release of cancer cells utilizing a long DNA aptamer-modified device. Reprinted with permission from ref. 129. Copyright 2012, National Academy of Sciences.

introduced to the device for 10 min at 37 °C, 68 ± 6% of the captured cells were released and about 66 ± 6% of cells retained a high viability.[129] Furthermore, Li *et al.* developed a hydrogel-coating device to specifically capture and non-destructively release CTCs.[106] The capture density was over 1000 cells per mm^2 using an aptamer-functionalized hydrogel coating, and only 5–15 cells per mm^2 of nonspecific binding was observed on the hydrogel surface. To release the captured cells from the hydrogel surface, restriction endonucleases were added to hydrolyze the aptamer sequences. The release efficiency reached 99%, and 98% of the released cells maintained a high viability.[106]

The above-mentioned methods exhibited excellent release efficiency for the captured CTCs with a high cell viability. However, some challenges still remain, such as the selection of optimal experimental conditions for the different aptamer sequences, and a long processing time, which have limited further applications. Therefore, cell release methods with high cell viability and easy operation remain a focus of attention.

6. Outlook

CTCs play a critical role in metastatic development and clinical diagnostics.[6–12] Therefore, it has become increasingly crucial to develop an efficient and reliable system for the enumeration and detection of CTCs. However, efficient isolation and accurate identification of CTCs remain challenging. The biggest difficulty is that CTCs are extraordinarily rare among a large population of hematological cells. Their heterogeneity makes it more difficult to isolate all CTCs. In addition, captured CTCs should remain viable and should be easily detached for downstream characterization and analysis. The integration of antibodies

with nanostructures, such as nanopillars/nanowires,[31–33] nanofibers,[34,35] nanoparticles,[36,37] nanotubes,[38,39] GO,[40] fractal nanostructures,[41] and nanorough-featured surfaces,[30] has been widely used in CTC capture. However, antibody-functionalized platforms have some disadvantages, including the need of a multistep fabrication process, high costs of the antibodies, and damage to recovered cells.

Aptamers have great application potential in the detection of CTCs since they are easily synthesized and modified, and possess high affinity and selectivity for various targets. Their affinity is comparable with an antibody/antigen interaction. Over the past decade, plenty of aptamers have been developed against cancer cell biomarkers through the SELEX technology. Aptamer-functionalized nanomaterials have been used for the isolation and detection of CTCs. Nanoparticles are small in size, can easily be modified with ligands, and have a high surface-to-volume ratio. Aptamer-functionalized nanoparticles play an important role in the isolation of CTCs.[43,44] Aptamer-conjugated multifunctional nanoparticles show great value in cell separation, detection, and imaging.[77,79,87,95] Nanostructures can enhance the interaction between cancer cells and the substrate to increase the capture efficiency of CTCs. Microfluidics devices have several advantages, including a low footprint, small sample volume, low reagent usage, and automatization, which make them suitable for the isolation of CTCs. However, the capture efficiency is limited for laminar flow, which may reduce the contact probability between cells and channels. Therefore, aptamer-modified nanostructure substrates have drawn increased attention.[96–98,100] Over the last decade, various microfluidic platforms have been developed. Phillips *et al.* reported an aptamer-functional microfluidic channel for the enrichment of cancer cells.[113] Aptamer cocktails and multiple aptamer combination systems were developed to efficiently isolate cancer cells with different phenotypes.[32] In addition, multifunctional chips have been proposed to realize the capture and analysis of CTCs.[123] Furthermore, captured cells can be released without damage under gentle conditions, which involved a change in secondary structure of the aptamers *via* nuclease degradation[106,129] or complementary sequence displacement.[101,138–140] The application of aptamers is still limited; for example, they are highly sensitive to nucleases *in vivo* and can be easily degraded. In addition, the conformation of aptamers is easily changed in different environments, and the small size and molecular mass of aptamers allow them to be rapidly eliminated *via* the kidneys. To address these issues, most aptamers in clinical studies can be chemically modified by replacing the 2′ position with either a fluoro (F), amino (NH_2), or *O*-methyl (OCH_3) group, and by capping the 3′ end with an inverted thymidine to increase the nuclease resistance, while also enhancing binding affinity.[141] Moreover, in previous studies, spiegelmers (L-aptamers), which are the enantiomers of wild-type RNA aptamers (D-aptamers), have been reported to be intrinsically insensitive to nucleases and thus possess better physiological *in vivo* stability.[142] In addition, aptameric structural modulation has recently been reported to improve the physiological stability of aptamers for *in vivo* applications. Tan *et al.* developed a circular bivalent aptamer for cancer cell recognition and *in vivo* tumor imaging. Subsequently, a supramolecular method was used to modulate the interaction between the circular bivalent aptamer and molecular therapeutics.[143,144]

The combination of multiple functional components is very promising. Taking advantage of both the aptamer and the nanostructure has shown great potential in the detection of CTCs. However, there are still some challenges that remain, including the interaction between CTCs and the nanostructure, the heterogeneity of CTCs, development of multifunctional devices, and the recovery of viable cells. To solve these problems, additional future studies are warranted.

Conflicts of interest

The authors declare no conflict of interest.

Acknowledgements

This work was financially supported by the National Natural Science Foundation of China (no. 21904135, 21775160), the Natural Science Foundation of Jiangsu Province (no. BK20180250), the CAS International Cooperation Key program (no. 121E32KYSB20170025), the Jiangsu Province Six Talent Peaks program and the CAS/SAFEA International Innovation Teams program.

References

1 S. C. Williams, *Proc. Natl. Acad. Sci. U. S. A.*, 2013, **110**, 4861.
2 C. Alix-Panabieres and K. Pantel, *Clin. Chem.*, 2013, **59**, 110–118.
3 P. S. Steeg and D. Theodorescu, *Nat. Clin. Pract. Oncol.*, 2008, **5**, 206–219.
4 P. S. Steeg, *Nat. Med.*, 2006, **12**, 895–904.
5 Y. Zhao, D. Xu and W. Tan, *Integr. Biol.*, 2017, **9**, 188–205.
6 P. Gazzaniga, E. de Berardinis, C. Raimondi, A. Gradilone, G. M. Busetto, E. De Falco, C. Nicolazzo, R. Giovannone, V. Gentile, E. Cortesi and K. Pantel, *Int. J. Cancer*, 2014, **135**, 1978–1982.
7 M. Cristofanilli, D. F. Hayes, G. T. Budd, M. J. Ellis, A. Stopeck, J. M. Reuben, G. V. Doyle, J. Matera, W. J. Allard, M. C. Miller, H. A. Fritsche, G. N. Hortobagyi and L. W. Terstappen, *J. Clin. Oncol.*, 2005, **23**, 1420–1430.
8 G. T. Budd, M. Cristofanilli, M. J. Ellis, A. Stopeck, E. Borden, M. C. Miller, J. Matera, M. Repollet, G. V. Doyle, L. W. Terstappen and D. F. Hayes, *Clin. Cancer Res.*, 2006, **12**, 6403–6409.
9 M. Cristofanilli, G. T. Budd, M. J. Ellis, A. Stopeck, J. Matera, M. C. Miller, J. M. Reuben, G. V. Doyle, W. J. Allard, L. W. Terstappen and D. F. Hayes, *N. Engl. J. Med.*, 2004, **351**, 781–791.
10 M. Yu, A. Bardia, N. Aceto, F. Bersani, M. W. Madden, M. C. Donaldson, R. Desai, H. Zhu, V. Comaills, Z. Zheng,

B. S. Wittner, P. Stojanov, E. Brachtel, D. Sgroi, R. Kapur, T. Shioda, D. T. Ting, S. Ramaswamy, G. Getz, A. J. Iafrate, C. Benes, M. Toner, S. Maheswaran and D. A. Haber, *Science*, 2014, **345**, 216–220.

11 E. A. Punnoose, S. Atwal, W. Liu, R. Raja, B. M. Fine, B. G. Hughes, R. J. Hicks, G. M. Hampton, L. C. Amler, A. Pirzkall and M. R. Lackner, *Clin. Cancer Res.*, 2012, **18**, 2391–2401.

12 C. Y. Lu, H. L. Tsai, Y. H. Uen, H. M. Hu, C. W. Chen, T. L. Cheng, S. R. Lin and J. Y. Wang, *Br. J. Cancer*, 2013, **108**, 791–797.

13 J. Loh, L. Jovanovic, M. Lehman, A. Capp, D. Pryor, M. Harris, C. Nelson and J. Martin, *J. Cancer Res. Clin. Oncol.*, 2014, **140**, 2157–2162.

14 W. J. Allard, J. Matera, M. C. Miller, M. Repollet, M. C. Connelly, C. Rao, A. G. Tibbe, J. W. Uhr and L. W. Terstappen, *Clin. Cancer Res.*, 2004, **10**, 6897–6904.

15 Y. Xiao, M. Shen and X. Shi, *J. Mater. Chem. B*, 2018, **6**, 1420–1432.

16 N. N. Lu, M. Xie, J. Wang, S. W. Lv, J. S. Yi, W. G. Dong and W. H. Huang, *ACS Appl. Mater. Interfaces*, 2015, **7**, 8817–8826.

17 X. Yu, R. He, S. Li, B. Cai, L. Zhao, L. Liao, W. Liu, Q. Zeng, H. Wang, S. S. Guo and X. Z. Zhao, *Small*, 2013, **9**, 3895–3901.

18 I. J. Fidler, *Hum. Vaccines Immunother.*, 2012, **8**, 1141–1142.

19 A. A. Powell, A. H. Talasaz, H. Zhang, M. A. Coram, A. Reddy, G. Deng, M. L. Telli, R. H. Advani, R. W. Carlson, J. A. Mollick, S. Sheth, A. W. Kurian, J. M. Ford, F. E. Stockdale, S. R. Quake, R. F. Pease, M. N. Mindrinos, G. Bhanot, S. H. Dairkee, R. W. Davis and S. S. Jeffrey, *PLoS One*, 2012, **7**, 33788–33799.

20 M. A. Nieto, R. Y. Huang, R. A. Jackson and J. P. Thiery, *Cell*, 2016, **166**, 21–45.

21 A. J. Armstrong, M. S. Marengo, S. Oltean, G. Kemeny, R. L. Bitting, J. D. Turnbull, C. I. Herold, P. K. Marcom, D. J. George and M. A. Garcia-Blanco, *Mol. Cancer Res.*, 2011, **9**, 997–1007.

22 H. Liu, Z. Ao, B. Cai, X. Shu, K. Chen, L. Rao, C. Luo, F.-B. Wang, W. Liu, M. Bondesson, S. Guo and F. Guo, *Nano Futures*, 2018, **2**, 025004.

23 H. Liu, X. Yu, B. Cai, S. You, Z. He, Q. Huang, L. Rao, S. Li, C. Liu, W. Sun, W. Liu, S. Guo and X. Zhao, *Appl. Phys. Lett.*, 2015, **106**, 093703.

24 W. Li, R. Li, B. Huang, Z. Wang, Y. Sun, X. Wei, C. Heng, W. Liu, M. Yu, S. S. Guo and X. Z. Zhao, *Nanotechnology*, 2019, **30**, 335101.

25 C. Alix-Panabieres and K. Pantel, *Nat. Rev. Cancer*, 2014, **14**, 623–631.

26 M. Yu, S. Stott, M. Toner, S. Maheswaran and D. A. Haber, *J. Cell Biol.*, 2011, **192**, 373–382.

27 B. Panchapakesan, R. Caprara, V. Velasco, J. Loomis, B. King, P. Xu, T. Burkhead, P. Sethu, L. J. Stallons, W. G. McGregor, S. N. Rai, G. Kloecker and E. Wickstrom, *Cancer Nanotechnol.*, 2010, **1**, 3–11.

28 W. J. Allard, J. Matera, M. C. Miller, M. Repollet, M. C. Connelly, C. Rao, A. G. J. Tibbe, J. W. Uhr and L. W. M. M. Terstappen, *Clin. Cancer Res.*, 2004, **10**, 6897–6904.

29 S. J. Cohen, C. J. A. Punt, N. Iannotti, B. H. Saidman, K. D. Sabbath, N. Y. Gabrail, J. Picus, M. A. Morse, E. Mitchell, M. C. Miller, G. V. Doyle, H. Tissing, L. W. Terstappen and N. J. Meropol, *Ann. Oncol.*, 2009, **20**, 1223–1229.

30 T. Kurihara, T. Itoi, A. Sofuni, F. Itokawa, T. Tsuchiya, S. Tsuji, K. Ishii, N. Ikeuchi, A. Tsuchida, K. Kasuya, T. Kawai, Y. Sakai and F. Moriyasu, *J. Hepatobiliary Pancreat. Surg.*, 2008, **15**, 189–195.

31 S. K. Lee, D. J. Kim, G. Lee, G. S. Kim, M. Kwak and R. Fan, *Biosens. Bioelectron.*, 2014, **54**, 181–188.

32 Q. Shen, L. Xu, L. Zhao, D. Wu, Y. Fan, Y. Zhou, W. H. Ouyang, X. Xu, Z. Zhang, M. Song, T. Lee, M. A. Garcia, B. Xiong, S. Hou, H. R. Tseng and X. Fang, *Adv. Mater.*, 2013, **25**, 2368–2373.

33 S. Wang, H. Wang, J. Jiao, K. J. Chen, G. E. Owens, K. Kamei, J. Sun, D. J. Sherman, C. P. Behrenbruch, H. Wu and H. R. Tseng, *Angew. Chem., Int. Ed.*, 2009, **48**, 8970–8973.

34 N. Zhang, Y. Deng, Q. Tai, B. Cheng, L. Zhao, Q. Shen, R. He, L. Hong, W. Liu, S. Guo, K. Liu, H. R. Tseng, B. Xiong and X. Z. Zhao, *Adv. Mater.*, 2012, **24**, 2756–2760.

35 S. Hou, L. Zhao, Q. Shen, J. Yu, C. Ng, X. Kong, D. Wu, M. Song, X. Shi, X. Xu, W. H. OuYang, R. He, X. Z. Zhao, T. Lee, F. C. Brunicardi, M. A. Garcia, A. Ribas, R. S. Lo and H. R. Tseng, *Angew. Chem., Int. Ed.*, 2013, **52**, 3379–3383.

36 R. He, L. Zhao, Y. Liu, N. Zhang, B. Cheng, Z. He, B. Cai, S. Li, W. Liu, S. Guo, Y. Chen, B. Xiong and X. Z. Zhao, *Biomed. Microdevices*, 2013, **15**, 617–626.

37 S. Jeon, W. Hong, E. S. Lee and Y. Cho, *Theranostics*, 2014, **4**, 1123–1132.

38 G. D. Chen, F. Fachin, M. Fernandez-Suarez, B. L. Wardle and M. Toner, *Small*, 2011, **7**, 1061–1067.

39 M. Abdolahad, M. Taghinejad, H. Taghinejad, M. Janmaleki and S. Mohajerzadeh, *Lab Chip*, 2012, **12**, 1183–1190.

40 H. J. Yoon, T. H. Kim, Z. Zhang, E. Azizi, T. M. Pham, C. Paoletti, J. Lin, N. Ramnath, M. S. Wicha, D. F. Hayes, D. M. Simeone and S. Nagrath, *Nat. Nanotechnol.*, 2013, **8**, 735–741.

41 P. Zhang, L. Chen, T. Xu, H. Liu, X. Liu, J. Meng, G. Yang, L. Jiang and S. Wang, *Adv. Mater.*, 2013, **25**, 3566–3570.

42 W. Chen, S. Weng, F. Zhang, S. Allen, X. Li, L. Bao, R. H. Lam, J. A. Macoska, S. D. Merajver and J. Fu, *ACS Nano*, 2013, **7**, 566–575.

43 Y. Chen, D. Tyagi, M. Lyu, A. J. Carrier, C. Nganou, B. Youden, W. Wang, S. Cui, M. Servos, K. Oakes, S. He and X. Zhang, *Anal. Chem.*, 2019, **91**, 4017–4022.

44 Z. Wang, W. Qin, J. Zhuang, M. Wu, Q. Li, C. Fan and Y. Zhang, *ACS Appl. Mater. Interfaces*, 2019, **11**, 12244–12252.

45 H. Dong, D. Yao, Q. Zhou, L. Zhang and Y. Tian, *Chem. Commun.*, 2019, **55**, 1730–1733.

46 T. Li, N. Li, Y. Ma, Y. J. Bai, C. M. Xing and Y. K. Gong, *J. Mater. Chem. B*, 2019, **7**, 6087–6098.

47 A. D. Hughes, J. Mattison, L. T. Western, J. D. Powderly, B. T. Greene and M. R. King, *Clin. Chem.*, 2012, **58**, 846–853.

48 G. Gakhar, V. N. Navarro, M. Jurish, G. Y. Lee, S. T. Tagawa, N. H. Akhtar, M. Seandel, Y. Geng, H. Liu, N. H. Bander, P. Giannakakou, P. J. Christos, M. R. King and D. M. Nanus, *PLoS One*, 2013, **8**, e85143.
49 M. J. Mitchell, C. A. Castellanos and M. R. King, *J. Biomed. Mater. Res., Part A*, 2015, **103**, 3407–3418.
50 H. Liu, Y. Li, K. Sun, J. Fan, P. Zhang, J. Meng, S. Wang and L. Jiang, *J. Am. Chem. Soc.*, 2013, **135**, 7603–7609.
51 L. Nie, F. Li, X. Huang, Z. P. Aguilar, Y. A. Wang, Y. Xiong, F. Fu and H. Xu, *ACS Appl. Mater. Interfaces*, 2018, **10**, 14055–14062.
52 G. Xu, Y. Tan, T. Xu, D. Yin, M. Wang, M. Shen, X. Chen, X. Shi and X. Zhu, *Biomater. Sci.*, 2017, **5**, 752–761.
53 L. Yang, H. Sun, W. Jiang, T. Xu, B. Song, R. Peng, L. Han and L. Jia, *Chem. Mater.*, 2018, **30**, 4372–4382.
54 H. Ulrich, C. A. Trujillo, A. A. Nery, J. M. Alves, P. Majumder, R. R. Resende and A. H. Martins, *Comb. Chem. High Throughput Screening*, 2006, **9**, 619–632.
55 A. D. Ellington and J. W. Szostak, *Nature*, 1990, **346**, 818–822.
56 C. Tuerk and L. Gold, *Science*, 1990, **249**, 505–510.
57 L. C. Bock, L. C. Griffin, J. A. Latham, E. H. Vermaas and J. J. Toole, *Nature*, 1992, **355**, 564–566.
58 L. Chen, F. Rashid, A. Shah, H. M. Awan, M. Wu, A. Liu, J. Wang, T. Zhu, Z. Luo and G. Shan, *Proc. Natl. Acad. Sci. U. S. A.*, 2015, **112**, 10002–10007.
59 X. Lou, J. Qian, Y. Xiao, L. Viel, A. E. Gerdon, E. T. Lagally, P. Atzberger, T. M. Tarasow, A. J. Heeger and H. T. Soh, *Proc. Natl. Acad. Sci. U. S. A.*, 2009, **106**, 2989–2994.
60 K. A. Yang, R. Pei and M. N. Stojanovic, *Methods*, 2016, **106**, 58–65.
61 F. Groher and B. Suess, *Methods*, 2016, **106**, 42–50.
62 H. X. Shi, W. W. Xiang, C. Liu, H. F. Shi, Y. Zhou and L. Gao, *Nanosci. Nanotechnol. Lett.*, 2018, **10**, 1707–1712.
63 Y. Liu, Y. X. Lai, G. J. Yang, C. L. Tang, Y. Deng, S. Li and Z. L. Wang, *J. Biomed. Nanotechnol.*, 2017, **13**, 1253–1259.
64 M. Q. Gu, J. L. Liu, D. L. Li, M. Wang, K. N. Chi, X. Zhang, Y. Deng, Y. C. Ma, R. Hu and Y. H. Yang, *Nanosci. Nanotechnol. Lett.*, 2019, **11**, 1139–1144.
65 Y. Liu, Y. Deng, T. Li, Z. Chen, H. Chen, S. Li and H. Liu, *J. Biomed. Nanotechnol.*, 2018, **14**, 2156–2161.
66 M. Liu, A. Khan, Z. Wang, Y. Liu, G. Yang, Y. Deng and N. He, *Biosens. Bioelectron.*, 2019, **130**, 174–184.
67 S. Li, H. Xu, H. Ding, Y. Huang, X. Cao, G. Yang, J. Li, Z. Xie, Y. Meng, X. Li, Q. Zhao, B. Shen and N. Shao, *J. Pathol.*, 2009, **218**, 327–336.
68 C. Wang, M. Zhang, G. Yang, D. Zhang, H. Ding, H. Wang, M. Fan, B. Shen and N. Shao, *J. Biotechnol.*, 2003, **102**, 15–22.
69 D. Shangguan, Y. Li, Z. Tang, Z. C. Cao, H. W. Chen, P. Mallikaratchy, K. Sefah, C. J. Yang and W. Tan, *Proc. Natl. Acad. Sci. U. S. A.*, 2006, **103**, 11838–11843.
70 J. P. Dassie, L. I. Hernandez, G. S. Thomas, M. E. Long, W. M. Rockey, C. A. Howell, Y. Chen, F. J. Hernandez, X. Y. Liu, M. E. Wilson, L. A. Allen, D. A. Vaena, D. K. Meyerholz and P. H. Giangrande, *Mol. Ther.*, 2014, **22**, 1910–1922.
71 S. E. Lupold, B. J. Hicke, Y. Lin and D. S. Coffey, *Cancer Res.*, 2002, **62**, 4029–4033.
72 H. S. Kang, Y. M. Huh, S. Kim and D. Lee, *Bull. Korean Chem. Soc.*, 2009, **30**, 1827–1831.
73 C. S. Ferreira, C. S. Matthews and S. Missailidis, *Tumour Biol.*, 2006, **27**, 289–301.
74 J. W. Kim, E. Y. Kim, S. Y. Kim, S. K. Byun, D. Lee, K. J. Oh, W. K. Kim, B. S. Han, S. W. Chi, S. C. Lee and K. H. Bae, *Mol. Cells*, 2014, **37**, 742–746.
75 Y. Song, Z. Zhu, Y. An, W. Zhang, H. Zhang, D. Liu, C. Yu, W. Duan and C. J. Yang, *Anal. Chem.*, 2013, **85**, 4141–4149.
76 J. Wang, Q. Wang, Y. Luo, T. Gao, Y. Zhao and R. Pei, *Talanta*, 2019, **204**, 424–430.
77 H. Jo, J. Her and C. Ban, *Biosens. Bioelectron.*, 2015, **71**, 129–136.
78 W. Sheng, T. Chen, W. Tan and Z. H. Fan, *ACS Nano*, 2013, **7**, 7067–7076.
79 J. X. Liu, N. Bao, X. Luo and S. N. Ding, *ACS Omega*, 2018, **3**, 8595–8604.
80 J. Xi and B. Zheng, *Nanosci. Nanotechnol. Lett.*, 2018, **10**, 309–319.
81 L. Rao, Q. F. Meng, Q. Huang, Z. Wang, G. T. Yu, A. Li, W. Ma, N. Zhang, S. S. Guo, X. Z. Zhao, K. Liu, Y. Yuan and W. Liu, *Adv. Funct. Mater.*, 2018, **28**, 1803531.
82 D. M. Zhu, L. Wu, M. Suo, S. Gao, W. Xie, M. H. Zan, A. Liu, B. Chen, W. T. Wu, L. W. Ji, L. B. Chen, H. M. Huang, S. S. Guo, W. F. Zhang, X. Z. Zhao, Z. J. Sun and W. Liu, *Nanoscale*, 2018, **10**, 6014–6023.
83 S. Guo, J. Xu, M. Xie, W. Huang, E. Yuan, Y. Liu, L. Fan, S. Cheng, S. Liu, F. Wang, B. Yuan, W. Dong, X. Zhang, W. Huang and X. Zhou, *ACS Appl. Mater. Interfaces*, 2016, **8**, 15917–15925.
84 D. Yin, G. Xu, M. Wang, M. Shen, T. Xu, X. Zhu and X. Shi, *Colloids Surf., B*, 2017, **157**, 347–354.
85 J. K. Herr, J. E. Smith, C. D. Medley, D. Shangguan and W. Tan, *Anal. Chem.*, 2006, **78**, 2918–2924.
86 J. E. Smith, C. D. Medley, Z. Tang, D. Shangguan, C. Lofton and W. Tan, *Anal. Chem.*, 2007, **79**, 3075–3082.
87 C. Sun, R. Zhang, M. Gao and X. Zhang, *Anal. Bioanal. Chem.*, 2015, **407**, 8883–8892.
88 X. Hua, Z. Zhou, L. Yuan and S. Liu, *Anal. Chim. Acta*, 2013, **788**, 135–140.
89 P. Miao and Y. Tang, *Anal. Chem.*, 2019, **91**, 15187–15192.
90 S. Fang, C. Wang, J. Xiang, L. Cheng, X. J. Song, L. G. Xu, R. Peng and Z. Liu, *Nano Res.*, 2014, **7**, 1327–1336.
91 S. Guo, Y. Q. Chen, N. N. Lu, X. Y. Wang, M. Xie and W. P. Sui, *Nanotechnology*, 2014, **25**, 505603.
92 Z. Li, G. L. Wang, Y. Shen, N. N. Guo and N. Ma, *Adv. Funct. Mater.*, 2018, **28**, 1707152.
93 B. Yang, B. Chen, M. He, X. Yin, C. Xu and B. Hu, *Anal. Chem.*, 2018, **90**, 2355–2361.
94 W. Lu, S. R. Arumugam, D. Senapati, A. K. Singh, T. Arbneshi, S. A. Khan, H. Yu and P. C. Ray, *ACS Nano*, 2010, **4**, 1739–1749.
95 F. Zheng, Y. Cheng, J. Wang, J. Lu, B. Zhang, Y. Zhao and Z. Gu, *Adv. Mater.*, 2014, **26**, 7333–7338.
96 Y. Wang, F. Zhou, X. Liu, L. Yuan, D. Li, Y. Wang and H. Chen, *ACS Appl. Mater. Interfaces*, 2013, **5**, 3816–3823.

97 N. Sun, X. Li, Z. Wang, R. Zhang, J. Wang, K. Wang and R. Pei, *ACS Appl. Mater. Interfaces*, 2016, **8**, 12638–12643.
98 J. Li, C. Qi, Z. Lian, Q. Han, X. Wang, S. Cai, R. Yang and C. Wang, *ACS Appl. Mater. Interfaces*, 2016, **8**, 2511–2516.
99 L. L. Xue, Z. L. Lyu, Y. F. Luan, X. H. Xiong, J. J. Pan, G. J. Chen and H. Chen, *Polym. Chem.*, 2015, **6**, 3708–3715.
100 R. Li, F. F. Chen, H. Q. Liu, Z. X. Wang, Z. T. Zhang, Y. Wang, H. Cui, W. Liu, X. Z. Zhao, Z. J. Sun and S. S. Guo, *ACS Appl. Mater. Interfaces*, 2018, **10**, 16327–16334.
101 N. Sun, J. Wang, L. Ji, S. Hong, J. Dong, Y. Guo, K. Zhang and R. Pei, *Small*, 2015, **11**, 5444–5451.
102 N. Sun, M. Liu, J. Wang, Z. Wang, X. Li, B. Jiang and R. Pei, *Small*, 2016, **12**, 5090–5097.
103 L. Liu, K. Yang, H. Gao, X. Li, Y. Chen, L. Zhang, X. Peng and Y. Zhang, *Anal. Chem.*, 2019, **91**, 2591–2594.
104 S. Li, N. Chen, Z. Zhang and Y. Wang, *Biomaterials*, 2013, **34**, 460–469.
105 B. P. Viraka Nellore, R. Kanchanapally, A. Pramanik, S. S. Sinha, S. R. Chavva, A. Hamme 2nd and P. C. Ray, *Bioconjugate Chem.*, 2015, **26**, 235–242.
106 L. Cao, L. Cheng, Z. Zhang, Y. Wang, X. Zhang, H. Chen, B. Liu, S. Zhang and J. Kong, *Lab Chip*, 2012, **12**, 4864–4869.
107 Y. Lin, L. Jiang, Y. Huang, Y. Yang, Y. He, C. Lu and H. Yang, *Chem. Commun.*, 2019, **55**, 5387–5390.
108 D. Ou, D. Sun, Z. Liang, B. Chen, X. Lin and Z. Chen, *Sens. Actuators, B*, 2019, **285**, 398–404.
109 A. Y. Fu, C. Spence, A. Scherer, F. H. Arnold and S. R. Quake, *Nat. Biotechnol.*, 1999, **17**, 1109–1111.
110 J. A. Davis, D. W. Inglis, K. J. Morton, D. A. Lawrence, L. R. Huang, S. Y. Chou, J. C. Sturm and R. H. Austin, *Proc. Natl. Acad. Sci. U. S. A.*, 2006, **103**, 14779–14784.
111 L. R. Huang, E. C. Cox, R. H. Austin and J. C. Sturm, *Science*, 2004, **304**, 987–990.
112 W. C. Chang, L. P. Lee and D. Liepmann, *Lab Chip*, 2005, **5**, 64–73.
113 J. A. Phillips, Y. Xu, Z. Xia, Z. H. Fan and W. Tan, *Anal. Chem.*, 2009, **81**, 1033–1039.
114 F. Zhang, L. Wu, W. Nie, L. Huang, J. Zhang, F. Li and H. Y. Xie, *Anal. Chem.*, 2019, **91**, 15726–15731.
115 Y. Wan, J. Tan, W. Asghar, Y. T. Kim, Y. Liu and S. M. Iqbal, *J. Phys. Chem. B*, 2011, **115**, 13891–13896.
116 Y. Wan, Y. Liu, P. B. Allen, W. Asghar, M. A. Mahmood, J. Tan, H. Duhon, Y. T. Kim, A. D. Ellington and S. M. Iqbal, *Lab Chip*, 2012, **12**, 4693–4701.
117 Y. Wan, M. A. Mahmood, N. Li, P. B. Allen, Y. T. Kim, R. Bachoo, A. D. Ellington and S. M. Iqbal, *Cancer*, 2012, **118**, 1145–1154.
118 W. Sheng, T. Chen, R. Kamath, X. Xiong, W. Tan and Z. H. Fan, *Anal. Chem.*, 2012, **84**, 4199–4206.
119 L. Zhao, C. Tang, L. Xu, Z. Zhang, X. Li, H. Hu, S. Cheng, W. Zhou, M. Huang, A. Fong, B. Liu, H. R. Tseng, H. Gao, Y. Liu and X. Fang, *Small*, 2016, **12**, 1072–1081.
120 Y. Song, Y. Shi, M. Huang, W. Wang, Y. Wang, J. Cheng, Z. Lei, Z. Zhu and C. Yang, *Angew. Chem., Int. Ed.*, 2019, **58**, 2236–2240.
121 M. Liu, Z. Wang, T. Tan, Z. Chen, X. Mou, X. Yu, Y. Deng, G. Lu and N. He, *Theranostics*, 2018, **8**, 5772–5783.
122 M. F. Abate, S. Jia, M. G. Ahmed, X. Li, L. Lin, X. Chen, Z. Zhu and C. Yang, *Small*, 2019, **15**, 1804890.
123 S. J. Reinholt and H. G. Craighead, *Anal. Chem.*, 2018, **90**, 2601–2608.
124 U. Dharmasiri, S. Balamurugan, A. A. Adams, P. I. Okagbare, A. Obubuafo and S. A. Soper, *Electrophoresis*, 2009, **30**, 3289–3300.
125 Y. Zhang, Z. Wang, L. Wu, S. Zong, B. Yun and Y. Cui, *Small*, 2018, **14**, 1704433.
126 N. Sun, X. Li, Z. Wang, Y. Li and R. Pei, *Biosens. Bioelectron.*, 2018, **102**, 157–163.
127 X. Yu, L. He, M. Pentok, H. Yang, Y. Yang, Z. Li, N. He, Y. Deng, S. Li, T. Liu, X. Chen and H. Luo, *Nanoscale*, 2019, **11**, 15589–15595.
128 R. Huang, L. He, Y. Xia, H. Xu, C. Liu, H. Xie, S. Wang, L. Peng, Y. Liu, Y. Liu, N. He and Z. Li, *Small*, 2019, **15**, 1900735.
129 W. Zhao, C. H. Cui, S. Bose, D. Guo, C. Shen, W. P. Wong, K. Halvorsen, O. C. Farokhzad, G. S. Teo, J. A. Phillips, D. M. Dorfman, R. Karnik and J. M. Karp, *Proc. Natl. Acad. Sci. U. S. A.*, 2012, **109**, 19626–19631.
130 A. A. Adams, P. I. Okagbare, J. Feng, M. L. Hupert, D. Patterson, J. Gottert, R. L. McCarley, D. Nikitopoulos, M. C. Murphy and S. A. Soper, *J. Am. Chem. Soc.*, 2008, **130**, 8633–8641.
131 J. Zhu, T. Nguyen, R. Pei, M. Stojanovic and Q. Lin, *Lab Chip*, 2012, **12**, 3504–3513.
132 L. S. Cheung, X. Zheng, A. Stopa, J. C. Baygents, R. Guzman, J. A. Schroeder, R. L. Heimark and Y. Zohar, *Lab Chip*, 2009, **9**, 1721–1731.
133 J. A. Martin, J. A. Phillips, P. Parekh, K. Sefah and W. Tan, *Mol. BioSyst.*, 2011, **7**, 1720–1727.
134 Y. Xu, J. A. Phillips, J. Yan, Q. Li, Z. H. Fan and W. Tan, *Anal. Chem.*, 2009, **81**, 7436–7442.
135 H. J. Lee, J. H. Oh, J. M. Oh, J. M. Park, J. G. Lee, M. S. Kim, Y. J. Kim, H. J. Kang, J. Jeong, S. I. Kim, S. S. Lee, J. W. Choi and N. Huh, *Angew. Chem., Int. Ed.*, 2013, **52**, 8337–8340.
136 M. Wirkner, J. M. Alonso, V. Maus, M. Salierno, T. T. Lee, A. J. Garcia and A. del Campo, *Adv. Mater.*, 2011, **23**, 3907–3910.
137 Q. Bian, W. Wang, S. Wang and G. Wang, *ACS Appl. Mater. Interfaces*, 2016, **8**, 27360–27367.
138 M. Labib, B. Green, R. M. Mohamadi, A. Mepham, S. U. Ahmed, L. Mahmoudian, I. H. Chang, E. H. Sargent and S. O. Kelley, *J. Am. Chem. Soc.*, 2016, **138**, 2476–2479.
139 Z. Zhang, N. Chen, S. Li, M. R. Battig and Y. Wang, *J. Am. Chem. Soc.*, 2012, **134**, 15716–15719.
140 S. Guo, H. Y. Huang, X. J. Deng, Y. Q. Chen, Z. R. Jiang, M. Xie, S. M. Liu, W. H. Huang and X. Zhou, *Nano Res.*, 2018, **11**, 2592–2604.
141 J. Zhou and J. Rossi, *Nat. Rev. Drug Discovery*, 2017, **16**, 181–202.
142 A. Vater and S. Klussmann, *Curr. Opin. Drug Discovery Dev.*, 2003, **6**, 253–261.
143 H. Kuai, Z. Zhao, L. Mo, H. Liu, X. Hu, T. Fu, X. Zhang and W. Tan, *J. Am. Chem. Soc.*, 2017, **139**, 9128–9131.
144 Y. Jiang, X. Pan, J. Chang, W. Niu, W. Hou, H. Kuai, Z. Zhao, J. Liu, M. Wang and W. Tan, *J. Am. Chem. Soc.*, 2018, **140**, 6780–6784.

